TIME-DOMAIN ASTRONOMY: A HIGH ENERGY VIEW, ESAC, MADRID, 13–15 JUNE 2018

Complex Circumnuclear Structures in the Radio-Loud AGN Mkn 6

Alex Markowitz[1,2], Beatriz Mingo[3], & Martin Hardcastle[4]

[1]CAMK-PAN; [2]Univ. of California, San Diego; [3]Open Univ.; [4]Univ. of Hertfordshire

Summary

Mkn 6 is a radio-loud Seyfert with sustained, recurrent radio activity. Its jet may have recently changed direction, in which case the accretion structure may not be fully stabilized, and one might expect a complex and messy circumnuclear environment. Mkn 6's X-ray spectrum does in fact consistently display complex (multi-zone) and time-variable X-ray absorption (e.g., B. Mingo et al. 2011, ApJ, 731, 21).

Here, we present preliminary results from two new broadband *NuSTAR+Suzaku* and *NuSTAR+Swift* observations in 2015, including the first high-quality >10 keV spectra of this source. We disentangle line-of-sight X-ray-absorbing structures and X-ray-reflecting gas to expand upon previous results, e.g., Mingo et al. (2011). We derive a self-consistent baseline model that includes full-covering Compton-thin absorption ($N_H \sim 1-8\times10^{22}$ cm^{-2}), partial-covering Compton-medium absorption ($N_H \sim 0.6-6\times10^{23}$ cm^{-2}), and Compton-thick reflection ($N_H \sim 4\times10^{24}$ cm^{-2}), and is additionally applicable to archival *XMM-Newton* and *Chandra* spectra, 2001–9.

The Compton-thick component could be a distribution of gas that is tilted as to not intersect the line of sight to the nucleus. The partial-covering absorber is consistent with clouds or clumps, possibly BLR clouds. Recent X-ray studies (e.g., G. Risaliti et al. 2009, ApJ, 696, 160; G. Risaliti et al. 2011, MNRAS, 410, 1027; A. Markowitz et al. 2014, MNRAS, 439, 1403) have provided support for a new generation of clumpy-torus models (M. Elitzur & I. Shlosmann, 2006, ApJ, 648, L101), and our work extends this support in radio-loud Seyferts. Mkn 6 may thus be a radio-loud analog of NGC 1365, in that both sources host numerous clumps manifesting themselves in X-ray spectra.

Introduction to Mkn 6

Mkn 6 is a Sy 1.5 located 80 Mpc away, known for hosting a peculiar set of radio structures (M.J. Kukula et al. 1996, MNRAS, 280, 1283, P. Kharb et al. 2006, ApJ, 652, 177):

- 7.5 kpc (20") large radio bubbles, oriented NE/SW, roughly aligned with host gxy's minor axis
- 1.5 kpc radio bubbles (~ 4") oriented E/W, **perpendicular** to the larger bubbles
- a 1 kpc collimated jet, N/S. (~3") roughly aligned with [O III]-emitting gas

Kharb et al. (2006) noted that a jet ejection axis can be easily perturbed, e.g., by a disk warp or by accretion events, and forwarded a model in which the jet's direction over the last 10^6 yrs has precessed and even flipped 140° from NE/SW to W/E about 10^5 yr ago. A consequence of the changes in jet orientation is that the jet may interact with and churn up the matter in the molecular torus, creating a chaotic accretion environment.

Mkn 6 is the only other radio-loud AGN besides Cen A (E. Rivers et al. 2011, ApJ, 742, L29) whose X-ray spectrum shows complex N_H variability. Immler et al. (2003, AJ, 126, 153), Schurch et al. (2006, MNRAS, 371, 211), and Mingo et al. (2011) explored the multiple X-ray absorbers using *XMM-Newton* and *Chandra*. **Here, we present the first high-quality spectral data >10 keV, using new *NuSTAR* observations to disentangle absorption, X-ray continuum emission, and Compton reflection.**

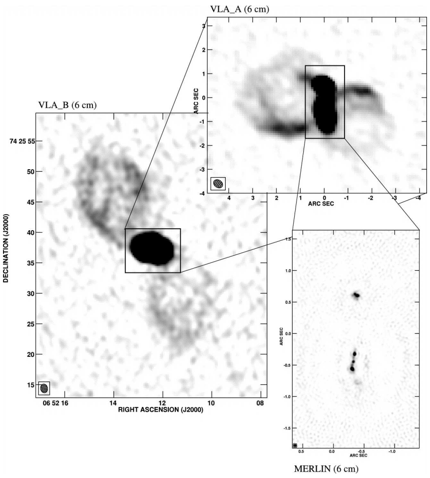

6 cm VLA/MERLIN images (Kharb et al. 2006 & Kukula et al. 1996)

Observations & Spectral Fitting Results

NuSTAR observed Mkn 6 simultaneously with *Suzaku* in April 2015, and simultaneously with *Swift*-XRT in November 2015, each yielding 0.5–50 keV spectra.

Our best-fit model uses MYTORUS components (Murphy & Yaqoob 2009, MNRAS, 397, 1549); our best fit has the form **Z90[A]*PL + S90[A]+L90[A]** + **Z90[B]*PL + S90[B]+L90[B]** + **S0[C] +L0[C].** "Z", "S", and "L" denote line-of-sight absorption, Compton reflection, and unresolved Fe Kα line emission, respectively. "90"/"0" denote inclination angles in/out of the line of sight. Component A is full-covering Compton-thin absorption. Component B is partial-covering Compton-medium gas, modifying a hard X-ray power-law (HXPL) dominating above ~ 10 keV. Component C is reflection from Compton-thick gas lying out of the line of sight; modeled in "decoupled" mode. Component C could also be modeled with blurred ionized reflection from a disk, but its flux does not track that of the HXPL (see below).

We also model a soft-Xray power law (SXPL) below 1.5 keV and a 0.9 keV APEC component to model thermal emission from the radio bubbles (Mingo et al. 2011).

From 2015 April to November, L_{2-50} increases by a factor of 1.75 (sum of hard power-laws illuminating components A & B). Best-fit covering fractions CF_B for component B are 77^{+8}_{-14}% and 62 ± 8%, respectively.

We applied our best-fit model to archival data: *XMM-Newton* and *Chandra*-ACIS observations spanning 2001 – 2009. To anchor the HXPL slope, and to include Compton-reflected emission from all components, we performed joint fits with 8–50 keV *NuSTAR* data, using whichever *NuSTAR* observation is closest in 3–10 keV flux, while allowing for the flux offsets. Results are summarized in Table 1.

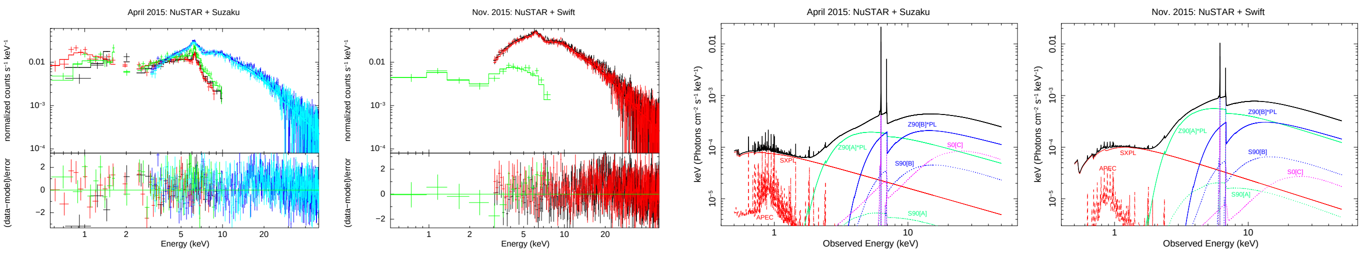

LEFT: Counts spectra for the 2015 April NuSTAR + Suzaku and 2015 November NuSTAR + Swift observations. **RIGHT:** Model components for our best-fitting MYTORUS model. Solid lines denote zeroth-order absorbed power-law components. Dashed lines denote reflection+line components. "A", "B", and "C" denote the Compton-thin, Compton-medium, & Compton-thick components.

Date	Instr.	F_{3-10} (erg cm^{-2} s^{-1})	$N_{H,A}$ (cm^{-2})	$N_{H,B}$ (cm^{-2})	Cov. Frac., B (CF_B)	Γ	L_{HXPL} (2–50 keV) (10^{43} erg s^{-1})
2015 Apr.	*NuSTAR* FPMA/B *Suzaku* XIS	4.3×10^{-12} (Nu.)	$8.5^{+1.4}_{-1.7}\times10^{22}$	$6.2\pm1.0\times10^{23}$	77^{+8}_{-14}%	$1.74^{+0.07}_{-0.09}$	3.15
2015 Nov.	*NuSTAR* FPMA/B *Swift* XRT	8.1×10^{-12} (Nu.)	$11.5^{+1.2}_{-1.5}\times10^{22}$†	6.2×10^{23}*	62 ± 8%	$1.83^{+0.04}_{-0.06}$	5.51
2001 Apr.	*XMM* EPIC^{+NuNov}	1.15×10^{-11} (pn)	$1.9^{+0.1}_{-0.5}\times10^{22}$	$0.84\pm0.11\times10^{23}$	65 ± 7%	1.82 ± 0.09	2.90
2003 Apr.	*XMM* EPIC^{+NuNov}	1.28×10^{-11} (pn)	$<1.2\times10^{22}$	$0.67^{+0.17}_{-0.13}\times10^{23}$	30^{+8}_{-7}%	1.83 ± 0.07	2.76
2005 Oct.	*XMM* EPIC^{+NuNov}	1.54×10^{-11} (pn)	$1.7\pm0.3\times10^{22}$	$0.63\pm0.11\times10^{23}$	68^{+8}_{-9}%	1.87 ± 0.10	3.52
2009 Jun.	*Chandra* ACIS^{+NuApr}	4.9×10^{-12} (Ch.)	$3.0\pm1.1\times10^{22}$	$2.9^{+0.4}_{-0.5}\times10^{23}$	93^{+4}_{-12}%	$1.77^{+0.11}_{-0.14}$	1.71

* = parameter held frozen.
† = large systematic errors present.
$^{+NuApr}$ or $^{+NuNov}$ denote simultaneous fits with the April or Nov. 2015 *NuSTAR* spectra.
$N_{H,C} = 4.0\times10^{24}$ for all fits (value held frozen for the 2015 Nov. *NuSTAR*, *XMM*, and *Chandra* spectra.)

Interpretation

- We interpret component B as **partial-covering clumps**. Their reflection component emanates from clouds on the far side of the SMBH. Column densities span ~ $0.6-6\times10^{23}$ cm^{-2}. Covering fraction measurements are usually 61 – 77%, but reach extremes of 30% & 93%. Because they only partially cover the X-ray corona, clouds must be < few tens of R_g in size (from $M_{BH} = 1.4\times10^8 M_\odot$, C.J. Grier et al. 2012, ApJ, 755, 60, e.g., 30 $R_g = 6\times10^{13}$ cm). Cloud number densities are thus likely of order $10^{9.5}$ cm^{-3}.

The clouds are likely close to the SMBH but are neutral or low-ionization; constraints on ionization parameter imply a distance r_{cloud} > 9 lt-dys. This limit is commensurate with the BLR's Hβ emission (9 – 10 lt-dys; Grier et al. 2012), but also encompasses the dusty torus (dust sublimation radius of 110–210 lt-days, from IR-reverberation mapping & IR interferometry; M. Kishimoto et al. 2011, A&A, 527A, 121).

We consider the clumpy-torus model of Nenkova et al. (2008, ApJ, 685, 160), in which clouds are preferentially distributed towards the equatorial plane, and our observations span a range of numbers of clouds in the line of sight. Given that CF_B is never observed to be 0% nor 100%, we're likely not seeing only one clump in any given observation — likely a few. If individual clouds each have typical covering fractions of (arbitrary values) 10% (30%), then XMM'03 (CF_B = 30%) corresponds to 4 (1) clouds along the line of sight; Chandra'09 (CF_B = 93%) corresponds to 25 (6) clouds. The remaining observations (CF_B = 61 – 77%) each correspond to 8–14 (2–3) clouds.

- The soft power-law is likely NOT leaked through component A: Its flux is roughly constant in time; $L_{0.5-2}$ spans $1.0-1.6\times10^{41}$ erg s^{-1} despite a factor of 3.4 variability in intrinsic L_{2-10}. It is likely scattered emission from optically-thin gas, $\tau \sim 0.01-0.02$; a possible origin is the kpc-scale Extended Narrow Line Region traced by [O III] (Kukula et al. 1996).
- Component A is **full-covering Compton-thin gas**, $N_H \sim 1-8\times10^{22}$ cm^{-2}; the range in values is likely due to systematic differences between instruments; its origin (close to the SMBH vs. associated with the host galaxy) is thus not clear.
- Component C denotes **Compton-thick matter**, $N_H \sim 4\times10^{24}$ cm^{-2}, which does NOT intersect the line of sight in any of the six observations. Although we cannot determine its exact morphology, a tilted donut or tilted cloud distribution is possible. The HXPL's current 2–50 keV luminosity is consistent with illuminating this component.

MAIN CONCLUSIONS

- We successfully applied a self-consistent absorption + reflection model to two newly-obtained joint *NuSTAR/Suzaku* and *NuSTAR/Swift* observations in 2015 plus archival CCD-quality data 2001–9. Our preferred model features full-covering Compton-thin absorption $N_{H,A} \sim 1-8\times10^{22}$ cm^{-2}, partial-covering Compton-medium gas ($N_{H,B} \sim 0.6-6\times10^{23}$ cm^{-2}; CF_B spanning 30 – 93%) but usually 62 – 77%), and reflection from Compton-thick gas ($N_{H,C} \sim 4\times10^{24}$ cm^{-2}) lying out of the line of sight.
- Spectral variability is primarily attributed to a combination of intrinsic variations in power-law (factor of 3.4) and in CF_B, and possibly mild variability in $N_{H,B}$.
- We attribute Component B to clumps near the SMBH, possibly BLR clouds. Mkn 6 is thus possibly a radio-loud analog to NGC 1365, which frequently displays exceptional X-ray spectral variability, and may benefit from a relatively favorable combination of geometry/viewing angle and/or a mechanism that produces numerous clouds.
- So far, all the clouds in Mkn 6 all have roughly similar values of $N_{H,B}$. However, if a set of Compton-thick clouds with high covering fractions were to traverse the line of sight, we could temporarily have a "changing-look" Seyfert.
- **Additional work in progress:** We will also test other solid-torus geometry models (Ikeda et al. 2009, ApJ, 692, 608; Brightman & Nandra, 2011, MNRAS, 413, 1206) as well as clumpy-torus reflection models (Liu & Li, 2014, ApJ, 787, 52; "BORUS", Baloković et al. 2018, ApJ, 854, 42).

•**ACKNOWLEDGEMENTS:** A.G.M. thanks T. Yaqoob for useful discussions on MYTORUS. A.G.M. acknowledges support from NASA Award NNX15AV13G and from Nardowe Centrum Nauki (NCN) award 2016/23/B/ST9/03123. B.M. acknowledges support from STFC grant ST/M001326/1. M.J.H. acknowledges support from STFC grant ST/M001008/1.